

## Electronic Supplementary Information:

### Many-Chain Effects on the Co-nonsolvency of Polymer Brushes in a Good Solvent Mixture

Gyehyun Park and YounJoon Jung\*

*Department of Chemistry, Seoul National University, Seoul 08826, Korea*

E-mail: yjjung@snu.ac.kr

#### Contents

1	System description . . . . .	Table S1
2	Maximum height of the brush . . . . .	Figure S1
3	Equilibrium bulk density as a function of the better solvent fraction . . . . .	Figure S2
4	Brush height as a function of chemical potential of the better solvent . . . . .	Figure S3
5	Density profile of free ends . . . . .	Figure S4
6	Density profiles of monomer and solvents at $x_b=0.3, 0.5, 0.7$ . . . . .	Figure S5
7	Parallel and perpendicular components of the radius of gyration . . . . .	Figure S6
8	Schematic description of the bond angle . . . . .	Figure S7
9	Unlooping probability . . . . .	Figure S8
10	Differential looping probability for the loop size . . . . .	Figure S9
11	Monomer coordination number of solvent . . . . .	Table S2

**Table S1.** System description:  $\sigma_g$ ,  $M$ ,  $N$ ,  $L_x$ ,  $L_y$ ,  $N_w$ , and  $N_{sol}$  are the grafting density, the number of grafted polymers, the degree of polymerization, the length of the system box along  $x$ -axis and  $y$ -axis, the number of wall atoms, and the number of solvent molecules, respectively.

$\sigma_g$	$M$	$N$	$L_x$	$L_y$	$N_w$	$N_{sol}$
0.002	1	50	25.00	21.65	400	12000
0.009	5	50	25.00	21.65	400	12000
0.019	10	50	25.00	21.65	400	12000
0.074	40	50	25.00	21.65	400	12000
0.148	80	50	25.00	21.65	400	12000
0.205	40	50	15.00	12.99	144	12000
0.308	60	50	15.00	12.99	144	12000
0.411	80	50	15.00	12.99	144	12000
0.001	1	100	37.50	32.48	900	50000
0.074	90	100	37.50	32.48	900	50000
0.148	180	100	37.50	32.48	900	50000

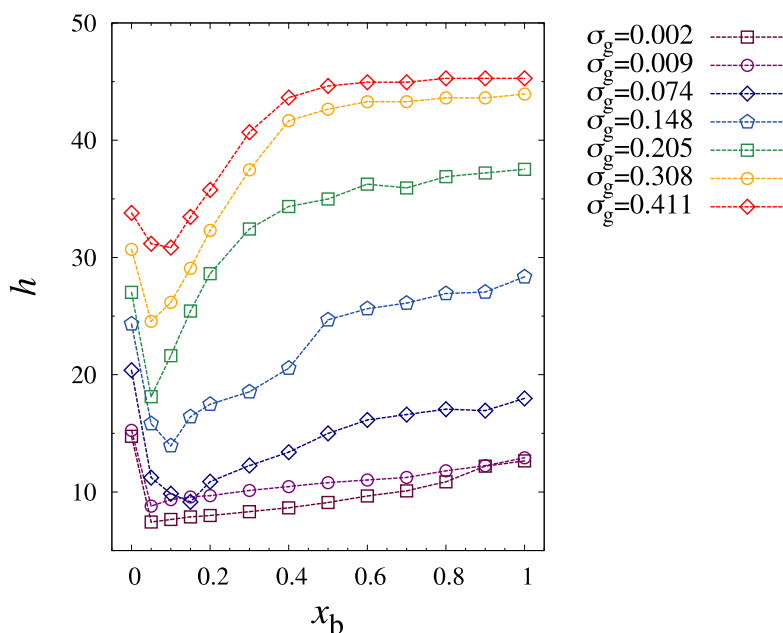


**Figure S1.** Maximum height of the brush as a function of the better solvent fraction for the various grafting densities. The maximum height is defined as the maximum value of  $z$  coordinate where the brush monomers exist. The better solvent fraction where the brush is in the maximally collapsed state varies for the grafting densities.

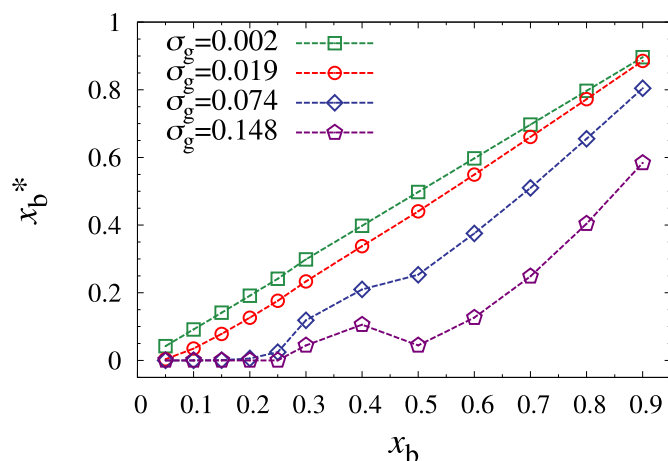


**Figure S2.** Equilibrium bulk density  $x_b^*$  as a function of a total better solvent fraction in the system  $x_b$ .  $x_b^*$  was calculated from the ratio of the number of better solvents and the total number of particles in bulk.

Comparison between the initial better solvent fraction ( $x_b$ ) and the equilibrium bulk density in the polymer-absent area ( $x_b^*$ ) is shown In **Figure S2** for the various grafting densities. The difference between  $x_b^*$  and  $x_b$  is notable when the co-nonsolvency occurs strongly and in the densely grafted polymer brush.

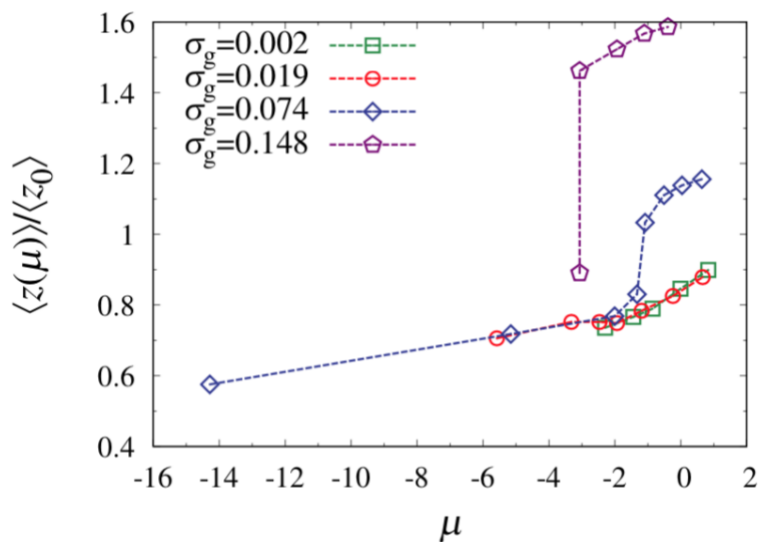


**Figure S3.** Brush height normalized with the height in the pure good solvent as a function of chemical potential of the better solvent in bulk for the two mushroom brushes ( $\sigma_g = 0.002, 0.019$ ) and the two overlapping brushes ( $\sigma_g = 0.074, 0.148$ ).

Based on the bulk density of the better solvent, we obtained the chemical potential of the better solvent defined as  $\mu = \ln(\rho/(1-\rho))$  and plotted the relative height of collapsed varying the chemical potential in the **Figure S3**. For the mushroom grafting density cases ( $\sigma_g = 0.002, 0.019$ ), the continuous change of relative brush height occurs as the chemical potential of better solvent decreases. Interestingly, the overlapping grafting density cases ( $\sigma_g = 0.074, 0.148$ ) show the discontinuous, first-order transition, and the discontinuity becomes more clear as the grafting density increases. The discontinuous and continuous transitions in the co-nonsolvency were also observed in the previous study, which reported that the transition behavior is affected by the selectivity of better solvent to monomers as well as the grafting density.[1]

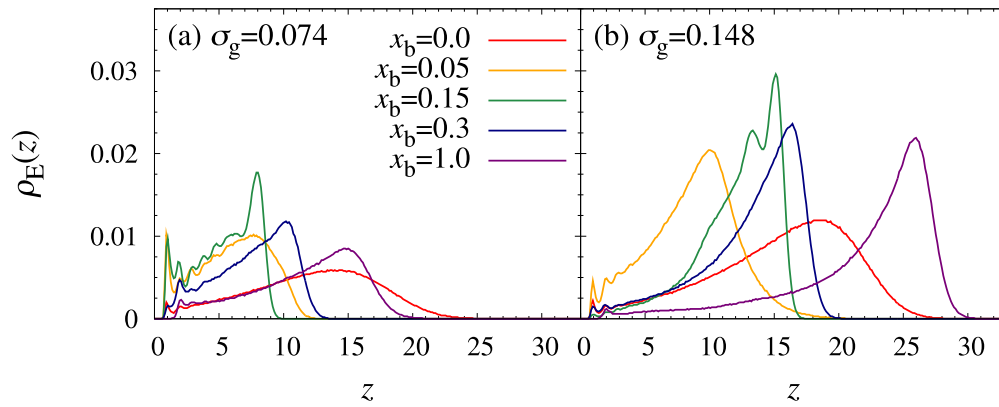


**Figure S4.** Density profile of the free ends in the chains for  $\sigma_g=0.074$  and  $\sigma_g = 0.148$  for the various better solvent fraction.

**Figure S4** shows the density profile of the monomer at the end of the chain. In pure solvent conditions, end monomers are present in a wide range of  $z$ . At  $x_b=0.1$ , a strong oscillation of the end monomer density is observed near the grafting wall. Local distribution of end monomer at  $x_b=0.1$  is entropically unstable, which suggests that co-nonsolvency is an entropically driven phenomenon. When polymer collapses in the mixture, the terminal monomers are more distributed near the wall in the case of  $\sigma_g=0.074$  than  $\sigma_g=0.148$ .

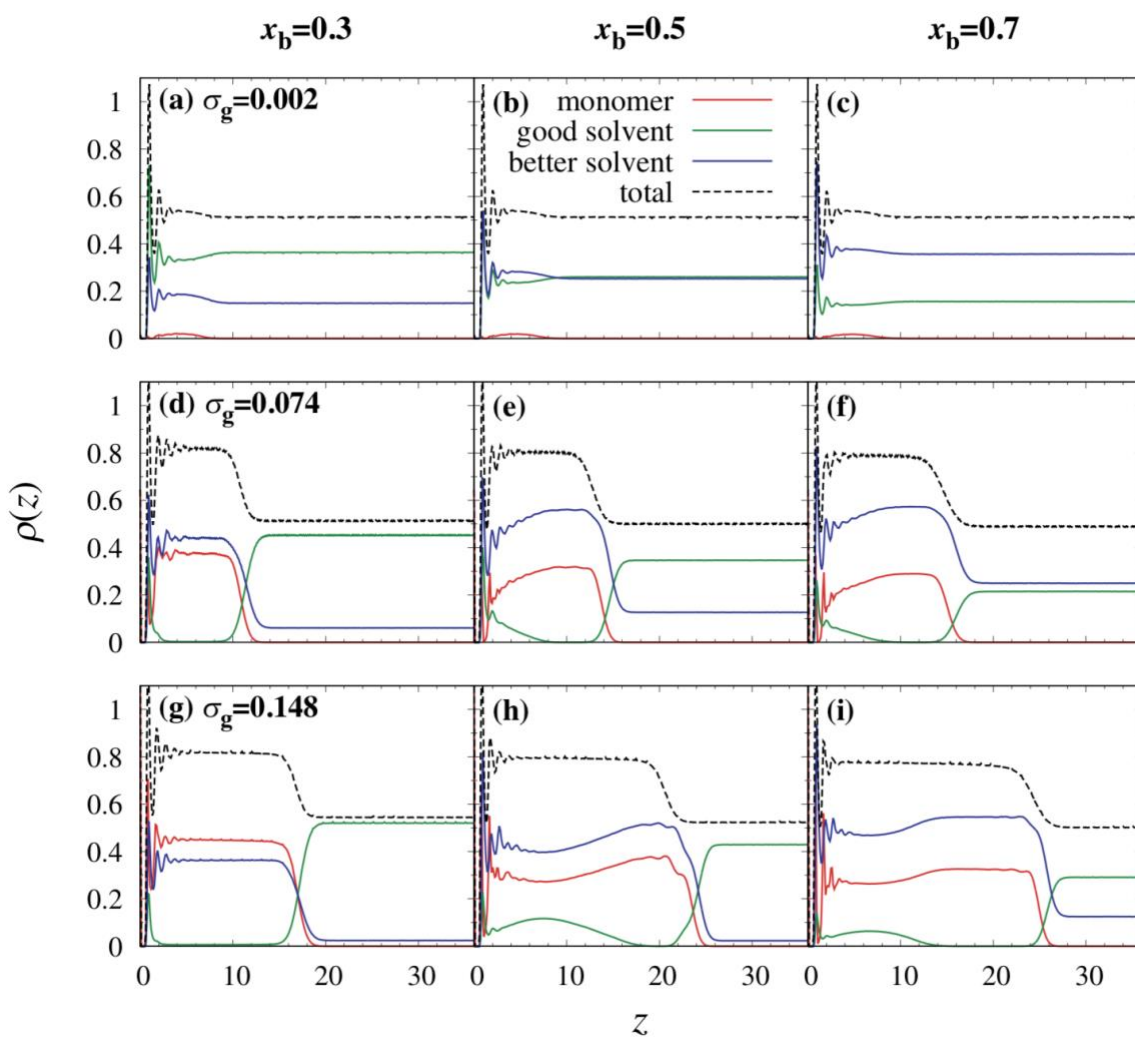


**Figure S5.** Density profile of the monomer, the good solvent, the better solvent and total particles (red, green, blue, and black dotted lines, respectively) as a function of vertical coordinate  $z$  at  $x_b = 0.3$  (left),  $x_b = 0.5$  (middle) and  $x_b = 0.7$  (right). The total density was calculated as the sum of monomer, good solvent and better solvent density. The graphs are present for three different grafting densities,  $\sigma_g = 0.002$  for (a), (b), and (c),  $\sigma_g = 0.074$  for (d), (e), and (f), and  $\sigma_g = 0.148$  for (g), (h), and (i).

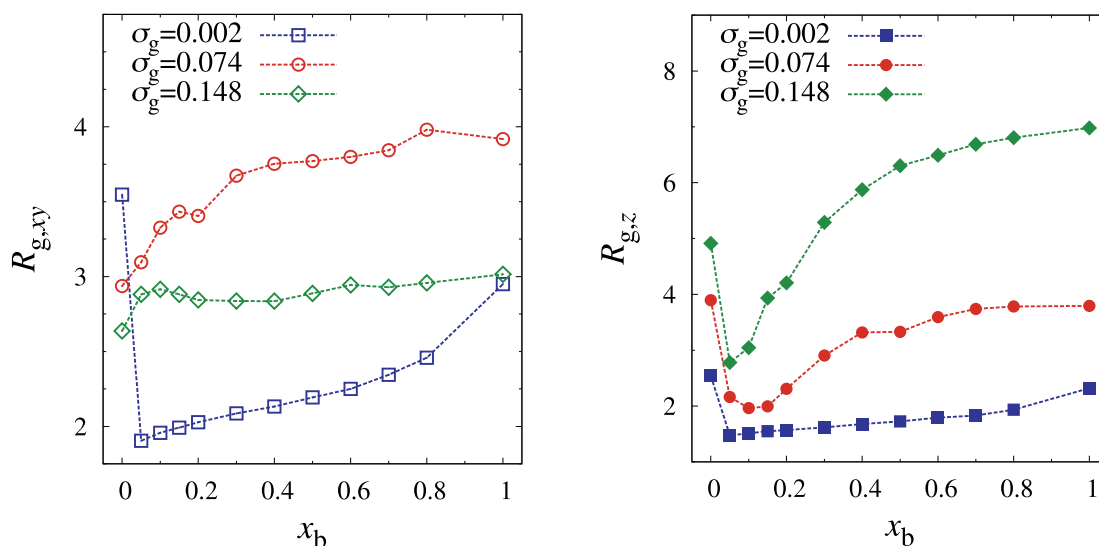


**Figure S6.** Parallel (left) and perpendicular (right) components of the radius of gyration for the three grafting surfaces. The point type represents the case of grafting density, and the line type represents the direction.

**Figure S6** shows the change in the radius of gyration of the polymer in three axial directions by varying the composition, which gives more information about the orientation of polymers. At  $\sigma_g=0.002$ , the change in orientation shows the same tendency along the solvent composition for the parallel and perpendicular directions. For  $\sigma_g=0.074$ , the magnitude of the parallel component and perpendicular component cross over when the solvent composition changes from  $x_b=0.0$  to  $x_b=0.1$ .

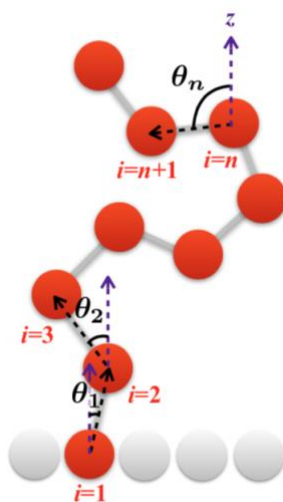


**Figure S7.** Schematic description of the bond angle  $\theta_n$  for a particular bond sequence number  $n$  in Eq. (9) in the main text. The black and purple dotted arrows represent the bond vector and the z-direction vector, respectively.

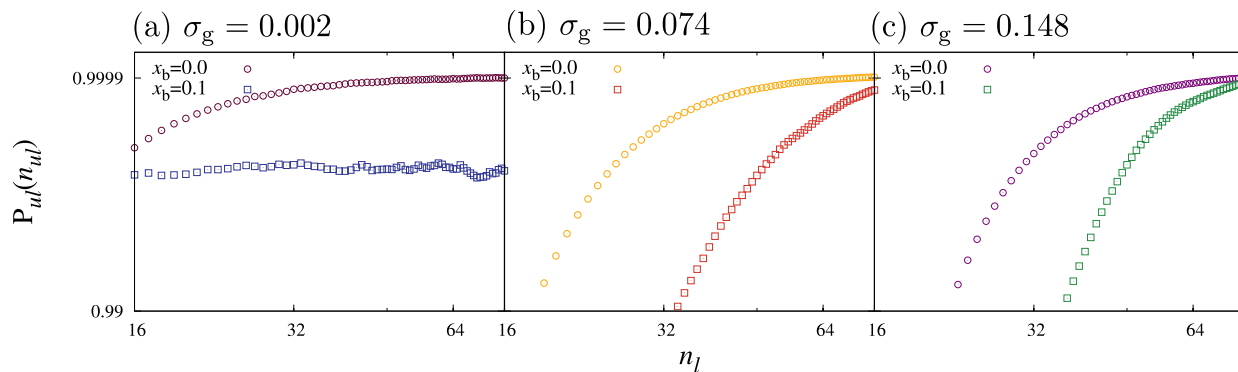


**Figure S8.** Unlooping probability distributions at  $x_b = 0.0$  and at  $x_b = 0.1$  for the lowest ( $\sigma_g = 0.002$ ), intermediate ( $\sigma_g = 0.074$ ), and highest grafting density ( $\sigma_g = 0.148$ ).

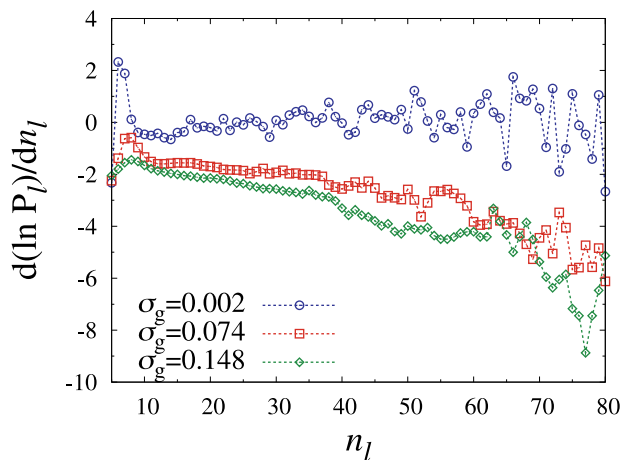


**Figure S9.** Differential looping probability at  $x_b = 0.1$  for the lowest ( $\sigma_g = 0.002$ ), intermediate ( $\sigma_g = 0.074$ ), and highest grafting density ( $\sigma_g = 0.148$ ).

$\sigma_g$	$N_c(x_b=0.0)$	$N_c(x_b=0.1)$	$N_c(x_b=0.1)/N_c(x_b=0.0)$
0.002	3.15	7.23	2.29
0.074	3.05	5.11	1.67
0.148	2.85	3.19	1.23

**Table S2.** Monomer coordination number of the solvent molecule in a pure solvent  $N_c(x_b=0.0)$ , in the mixture  $N_c(x_b=0.1)$ , and their ratio  $N_c(x_b=0.1)/N_c(x_b=0.0)$ .

In order to investigate in more detail the solvent molecule-assisted bridging structure formed by the monomers, the monomer coordination number of the solvent molecule is calculated on average. Here, the coordinated solvent is the one that contacts with monomers within the distance  $1.4\sigma$ . To eliminate the intrinsic crowding effect of the chains,  $N_c(x_b=0.1)$  is normalized to the value in a pure good solvent  $N_c(x_b=0.0)$ . As shown in **Table S2**, the relative proportion of the coordination number at  $x_b=0.1$  is the largest in the brush for  $\sigma_g=0.002$ . At  $\sigma_g=0.148$ , many-chain effects interfere with the multi-coordination of the co-solvent due to the chain repulsion.

## References

- [1] A. Galuschko, J.-U. Sommer, *Macromolecules*, 2019, **52**, 4120.